Cross-Linked Polyfluorene Polymer Precursors: Electrodeposition, PLED Device Characterization, and Two-Site Co-deposition with Poly(vinylcarbazole)

Seiji Inaoka,[†,§] Daniel B. Roitman,[*,†,∥] and Rigoberto C. Advincula[*,‡]

Agilent Technologies Laboratories, 3500 Deer Creek Road, Palo Alto, California 94304, and Department of Chemistry, University of Houston, Houston, Texas 77204

Received July 3, 2005. Revised Manuscript Received October 19, 2005

Electropolymerization of π-conjugated polymers is considered as an alternative method for depositing and patterning charge injection, transport, and luminescent layers in organic electronic devices. In this study, a series of novel poly(fluoren-9,9-diyl-*alt*-alkan-α,ω-diyl) polymers with increasing alkyl spacer lengths were synthesized and used as precursors for the deposition of conjugated polymers formed by the oxidative coupling of the fluorene units. The precursor polymers and their conjugated polymer network were characterized in solution and in film form, and their charge-transport characteristics were investigated by fabricating electroluminescent polymer light emitting diode (PLED) devices. Interesting charge carrier transport properties based on thickness and co-deposition with another precursor polymer gives the potential for optimized solid-state device performance and film processing conditions. Finally, a "two-pixel" prototype PLED was demonstrated using a sequential electrochemical co-deposition method with poly-(vinylcarbazole) (PVK).

Introduction

Developing processes for high-resolution lithographic patterning of polymer light emitting diode (PLED) devices and other organic electronic devices and sensors remains a challenge.[1] This challenge is due, in part, to difficulties involved in formulating electroluminescent and electroactive polymers with photoresist-compatible properties. This problem has been circumvented by elegant direct deposition methods, such as ink jet printing[2] and screen printing,[3] or by overlaying filters[4] and diffusing color dyes[5] in light emitting backplanes. While these approaches are adequate for relatively large features (tens of micrometers), they possess serious implementation limitations as the features approach the micrometer and sub-micrometer levels. Recently a group led by Müller et al.[6] successfully demonstrated high efficiency red−blue−green (RGB) photopatterned devices using novel derivatives of spirobifluorene-fluorene copolymers using oxetane reactive units as a cross-linker.

Another approach is to develop patterns by "directing" and "cross-linking" the active materials to predefined regions on the device without having to repeat cycles of mask aligning, baking, and lifting-off, which are processes usually associated with conventional photoresist technology. On the other hand, the electrochemical nanopatterning of poly(vinylcarbazole) (PVK), a well-known hole-injecting material, has recently been demonstrated.[7] In this paper, we report results toward achieving this protocol. Our group has explored the use of electrochemical polymerization (oxidation) as a "direct writing" method for depositing films in arbitrary patterns. If successful, multilayer and laterally resolved regions could be easily coated by sequential electrodeposition of precursor polymers and monomers by simply switching on-and-off different conducting paths during electropolymerization. This approach has the additional advantage of potentially achieving patterns with arbitrarily small features, limited only by the size of the underlying electrodes. Furthermore, the composition and properties of each layer or feature can be controlled separately by the selection of monomers and precursor compositions[8] as well as counterion-bound species (optical and/or electrical dopants), including polyelectrolytes, dyes, and charged micro- and nanoparticles.[9]

Electropolymerization has been shown to be an effective deposition method of thin films for a variety of conjugated polymers such as polypyrrole, polythiophene, and poly(3-alkylthiophene).[10] However, controlling polymer solubility and morphology are some of the challenges in achieving high-quality films. Typically a "poor" solvent is chosen for

(1) Holmes, A. *Nature* **2003**, *421*, 800.
(2) (a) Hebner, T. R.; Wu, C. C.; Marcy, D.; Lu, M. H.; Sturm, J. C. *Appl. Phys. Lett.* **1998**, *72*, 519. (b) Roitman, D. B. U.S. Pat. 5,972,-419, October 1999.
(3) Pardo, D. A.; Jabbour, G. E.; Peyghambarian, N. *Adv. Mater.* **2000**, *12*, 1249.
(4) Proano, R. E.; Misage, R. S.; Jones, D.; Ast, D. G. *IEEE Trans. Electron Devices* **1991**, *38*, 1781.
(5) (a) Pschenitzka, F.; Sturm, J. C. *Appl. Phys. Lett.* **1999**, *74*, 1913. (b) Chang, S.-C.; He, G.; Chen, F.-C.; Guo, T.-F.; Yang, Y. *Appl. Phys. Lett.* **2001**, *79*, 2088.
(6) Muller, C. D.; Falcou, A.; Reckefuss, N.; Rojahn, M.; Wiederhirn, V.; Rudati, P.; Frohne, H.; Nuyken, O.; Becker, H.; Meerholz, K. *Nature* **2003**, *421*, 829.

(7) Jegadesan, S.; Advincula, R. C.; Valiyaveettil, S. *Adv. Mater.* **2005**, *17*, 1282−1285.
(8) Roitman, D. B.; Inaoka, S.; Advincula, R. C. U.S. Pat. 6,294,245 (2001), 6,533,918B2 (2003), and 6,552,101B1 (2003).
(9) Ganopahyay, R.; De, A. *Chem. Mater.* **2000**, *12*, 608.

the polymer to be deposited in order to drive the oligomerized species out of solution and onto the electrode to form a film. This combination often results in poor film morphology (usually a fractured layer of oligomerized or polymerized conjugated species). Electropolymerization in "good" solvent conditions with standard electrochemical reagents, on the other hand, does not usually lead to film formation because in such solvents the polymers formed as the electrode diffuses back into the solution.

Fluorenes and its derivatives are materials used in fluorescence applications[11] and in organic light emitting devices.[12] Of high interest is the synthesis of conjugated fluorene polymers with fluoren-2,7-diyl units synthesized either by palladium- or nickel-catalyzed coupling of 2,7-dibromofluorenes,[13] Suzuki coupling between 2,7-dibromofluorene and 2,7-dioxaborolarylfluorene derivatives,[14] chemical oxidation of fluorenes with FeCl$_3$,[15] and electrochemical oxidation of fluorenes have been reported.[16] Our group has previously synthesized a series of novel linear "precursor" polymers with fluorene pendant groups along a flexible alkyl backbone (Figure 1).[17,22] The structure of these polymers is categorized as "class C" by Shirota et al.[18] It is expected that oxidation (either chemical or electrochemical) of this polymer should result in coupling between 2- and 2′-fluorenyl positions, forming oligofluorenyl units in a three-dimensional polymer network (Figure 2). This paper proposes that the electrochemical deposition of 2−2′ fluorenyl coupled electroactive polymers from the alkyl precursors (as well as other members of the class "C" family of polymers) can be achieved under good solvent conditions (for the precursor as well as for the electroactive polymer) because the reaction results in an extended cross-linked network structure. We have observed these films to exhibit excellent mechanical integrity and strength as a result of the combined intramolecular alkyl and intermolecular π-conjugated linkages. This is in sharp contrast with films obtained by conventional electropolymerization of "pure" main chain conjugated
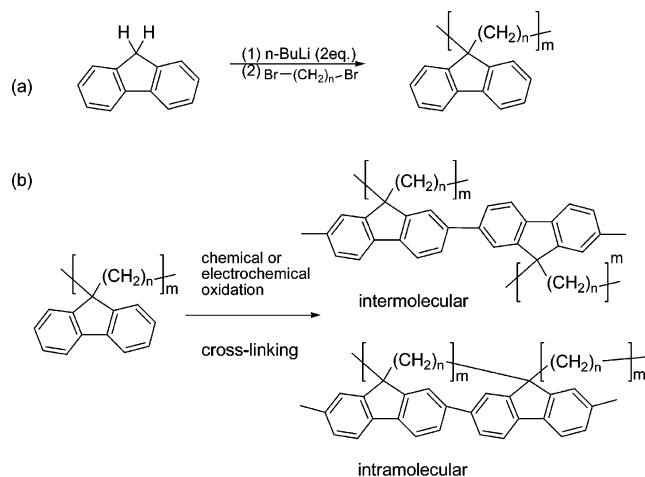

Figure 1. (a) Synthesis of fluorene-containing polymers with $n = 4$, 6, 8, 10, 12 or polymers **1a**, **1b**, **1c**, **1d**, **1e**, respectively. (b) Chemical or electrochemical oxidation leading to the formation of cross-linked or a conjugated polymer network.
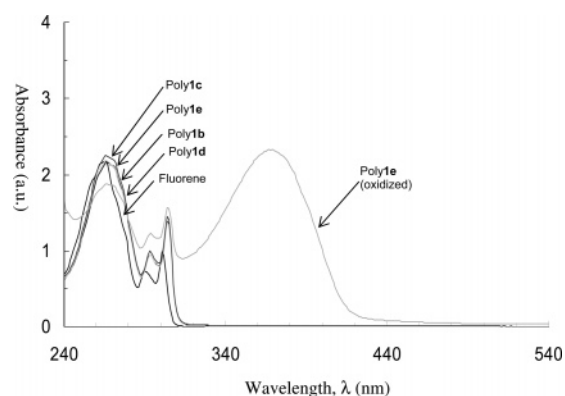

Figure 2. UV−vis spectra of polymers **1b**, **1c**, **1d**, **1e**, and **1e**(chemically oxidized) solution in CHCl$_3$.

polymers where the mechanical strength of the film is determined exclusively by the extent of polymerization along the π-conjugated backbone. A number of these precursor polymers have been previously reported by our group, and their excellent electropolymerizability and film properties have been reported.[19] In the first part, we discuss the characterization of fluorene-based precursor polymers and their oxidative conversion both in solution as well as electrochemically. In the second part we consider their behavior in electroluminescent devices. Finally, we demonstrate the feasibility of fabricating PLED's by the direct electrochemical patterning of films with different electronic characteristics on a single substrate.

Experimental Section

Materials. Fluorene, *n*-butyllithium (2.5 M solution in hexanes), 1,4-dibromobutane, 1,6-dibromohexane, 1,8-dibromooctane, 1,10-dibromodecane, 1,12-dibromododecane, iron(III) chloride, chlorobenzene, 3-octylthiophene, tetrabutylammonium tetrafluoroborate, poly(9-vinylcarbazole) (PVK, MW = 62 000) were purchased from Aldrich Chemical Co. and used without further purification. Diethyl ether (anhydrous; Fisher) was purified by distillation over sodium benzophenone ketyl. Methanol (anhydrous), acetonitrile (anhydrous), chloroform, and methylene chloride were purchased from Fisher Scientific and used without further purification. A high-performance green light polymer based on poly(dioctyllfluorene-

(10) (a) Street, G. B.; Clark, T. C.; Krounbi, K.; Pfluger, P.; Rabolt, J. F.; Geiss, R. H. *Polym. Prepr. (Am. Chem. Soc., Div. Polym. Chem.)* **1982**, *23*, 117. (b) Kaneto, K.; Kohno, Y.; Yoshino, K.; Inuishi, Y. *J. Chem. Soc., Chem. Commun.* **1983**, 382. (c) Glenis, S.; Tourillon, G.; Garnier, F. *Thin Solid Films* **1984**, *122*, 9. (d) Prejza, J.; Lundstrom, I.; Skotheim, T. *J. Electrochem. Soc.* **1982**, *129*, 1685.
(11) (a) Klaerner, G.; Miller, R. D. *Macromolecules* **1998**, *31*, 2007. (b) Yang, Y.; Pei, Q. *J. Appl. Phys.* **1997**, *81*, 3294.
(12) Bernius, M.; Inbasekaran, M.; O'Brien, J.; Wu, E. *Adv. Mater.* **2000**, *12*, 1737.
(13) Pei, Q.; Yang, Y. *J. Am. Chem. Soc.* **1996**, *118*, 7416.
(14) Ranger, M.; Rondeau, D.; Leclerc, M. *Macromolecules* **1997**, *30*, 7686.
(15) Fukuda, M.; Sawada, K.; Yoshino, K. *J. Polym. Sci., Part A: Polym. Chem.* **1993**, *31*, 2465.
(16) Hapiot, P.; Lagrost, C.; Le Floch, F.; Raoult, E.; Rault-Berthelot, J. *Chem. Mater.* **2005**, *17*, 2003.
(17) Park, M. K.; Xia, C.; Advincula, R. C.; Schutz, P.; Caruso, F. *Langmuir* **2001**, *17*, 7670.
(18) (a) Shirota, Y.; Nogami, T.; Noma, N.; Kakuta, T.; Saito, H. *Synth. Met.* **1991**, *41−43*, 1169. (b) Imae, I.; Nawa, K.; Ohsedo, Y.; Noma, N.; Shirota, Y. *Macromolecules* **1997**, *30*, 380. (c) Jeon, I.-R.; Noma, N.; Shirota, Y. *Bull. Chem. Soc. Jpn.* **1992**, *65*, 1062.
(19) (a) Deng, S.; Advincula, R. *Chem. Mater.* **2002**, *14*, 4073. (b) Taranekar, P.; Fan, X.; Advincula, R. *Langmuir* **2002**, *18*, 7943. (c) Xia, C.; Fan, X.; Park, M.; Advincula, R. *Langmuir* **2001**, *17*, 7893.
(20) He. Y.; Gong, R.; Kanicki, J. *Appl. Phys. Lett.* **1999**, *74*, 2265.
(21) (a) Ho, P. K. H.; Kim, J. S.; Burroughes, J.; Becker, H.; Li, S. F.; Brown, T. M.; Cacialli, F.; Friend, R. H. *Nature* **2000**, *404*, 481. (b) Millard, I. S. *Synth. Met.* **2000**, *111−112*, 119.
(22) Inaoka, S.; Advincula, R. C. *Macromolecules,* **2002**, *35*, 2426−2428.

Table 1. EL Behavior of Devices with Spin-Cast Polymers 1 as HT Layer

HT material	total thickness (nm) (HT thickness)	oxidation FeCl$_3$	V_{bias} (V) (E^a)	J (mA/cm^2)	L (Cd/m^2)	L/J (Cd/A)
none[b]	85 (0)	−	15.8 (1.9)	100	701	0.7
poly**1b**	89 (4)	no	10.7 (1.2)	10	62	0.63
poly**1b**	88 (3)	yes	9.0 (1.0)	20	270	1.57
poly**1c**	118 (33)	no	16.5 (1.4)	5	46	0.92
poly**1c**	96 (11)	yes	8.4 (0.9)	10	176	1.76
			15.9 (1.7)	100	1500	1.5
poly**1d**	121 (36)	no	12.9 (1.1)	10	155	1.56
poly**1d**	92 (7)	yes	9.5 (1.0)	10	231	2.31
poly**1e**	103 (17)	no	8.5 (1.1)	10	204	2
			14 (1.4)	100	2200	2.2
poly**1e**	118 (33)	yes	6.2 (0.5)	10	266	2.7
			10.2 (0.9)	100	2400	2.4
poly**1e**	96 (11)	c	8.5 (0.9)	10	204	2.04

^{a} E = average field strength in 10^6 V/cm. ^{b} BTF8 was spin-cast directly on ITO. ^{c} Soluble fraction of chemically oxidized poly**1e** with FeCl$_3$.

benzothiadiazole) (BTF8) was provided by the Dow Chemical Co. The composition of the sample used is proprietary. The EL characteristics of this class of polymers have been described by He [20] and by Friend and co-workers.[21] 3,4-Dioxyethylenethiophene (EDT) was purchased from Bayer Co. ITO-coated glass chips (15 mm × 15 mm) were purchased from Donelly Co.

Characterization. ^{1}H NMR analysis was carried out with Bruker spectrometer at 300 MHz. UV−vis measurements were carried out on a Perkin-Elmer Lambda 20. Fluorescence spectra were obtained in a Perkin-Elmer LS50B spectrometer using 320 nm excitation. Thermal transition behavior was investigated on a Mettler DSC 30 differential scanning calorimeter (DSC) at the rate of 10°/min. MALDI-TOF-MS analysis was carried out with a Perspective Biosystems Voyager Elite DE system. Gel permeation chromatography (GPC) characterization was carried out in tetrahydrofuran (THF) at 1 mL/min with Waters Styragel columns equipped with a Waters 410 differential refractometer detector. Polystyrene standards were used for calibration.

Synthesis. The polymers utilized in this study have been synthesized, characterized, and reported in a previous study.[22] In general, an S$_N$2 type substitution reaction was modified toward polymerization by lithiation reactions on the 9,9 position of fluorene followed by reaction with a series of α,ω-dibromoalkane with different chain lengths. This resulted in a polymer series where the fluorene units are separated by alkylene spacers, i.e., poly-(fluoren-9,9-diyl-*alt*-alkan-α,ω-diyl) homologous series. The details are further enumerated in the Supporting Information and another previous publication.[22]

Device Fabrication. (a) Spin-Cast Films. Preliminary studies involved spin casting the precursor films followed by chemical oxidation of the cast films in a solution of FeCl$_3$. The precursor polymers were spin cast from chlorobenzene solutions on ITO-coated glass. Concentrations and spinning rates were adjusted to obtain films with thickness of about 100 nm. After substrate drying on the spinner, the FeCl$_3$ solution in chlorobenzene was added dropwise to the substrate and was spun immediately for a second time. The reason for choosing cholorobenzene as solvent was to secure the full exposure of the oxidizing agent and solvent wetting to the existing polymer film. Afterward the substrates were washed away with 2-propanol (a better solvent to FeCl$_3$) to remove any excess oxidizing agent. However, the films showed considerable solvent erosion resulting in thicknesses of the order of 2.5 to 35 nm (HT thickness on Table 1).

(b) Electrodeposited Films. Electrochemical oxidation and deposition (ED) of precursor polymers on ITO-coated glass were carried out using Cypress Systems CS-1090 electrochemical analyzer with precursor polymer solution (50 mM in methylene chloride) with tetrabutylammonium tetrafluoroborate as supporting

electrolyte (100 mM). Cyclic voltammograms (CV) were recorded with a Cypress Systems EE009 reference electrode (Ag/AgCl) and EE011 platinum counter electrode. Film thickness (typically between 20 and 200 nm) was controlled by the number of cycles, sweep rate, and the voltage limits. The thickness was determined by atomic force microscopy (AFM) profilometry as previous described. Additional layers were deposited by standard spin-coating of polymer solutions at ca. 2000 rpm. Typical thickness was ca. 100 nm. Vacuum sublimation deposition of calcium cathode was carried out at the rate of 0.3 nm/s (at 10^{-7} Torr) in a Kurt Lesker vacuum chamber.

(c) PLED Device Characterization. Device characteristics analysis was carried out in a glovebox with nitrogen atmosphere rigorously dried. A photodiode detector and the devices were connected to an external Hewlett-Packard 4155A semiconductor analyzer, with which operating bias (V), current density (J), and luminance (L) or brightness (Cd/m^2) were digitally recorded. The EL spectra of the devices were not recorded.

Results and Discussion

Synthesis. A series of poly(fluoren-9,9-diyl-*alt*-alkan-α,ω-diyl) polymer was synthesized by dilithiation of fluorene at the 9,9 position, followed by an S$_N$2 substitution polymerization reaction of the intermediate with α,ω-dibromoalkane (Figure 1a).

An amorphous low molecular weight polymer that can be precipitated in methanol was the major product, when 9,9-dilithiofluorene is mixed with up to three times the equivalent of α,ω-dibromoalkane. The characterization by NMR revealed a statistical trend of peak shifts to the upfield especially with shorter alkyl chain lengths, i.e., $n = 4$, which imply the shielding effect by fluorene rings in the polymer. GPC based on polystyrene standards showed large variability in relative molecular weights (MW) and polydispersity index (PDI), suggesting that the propagation step of the polymerization conditions were not well-controlled. In principle, higher MWs and better distribution (PDI) can be obtained by using a more rigorous and optimized stoichiometric titration polymerization method. Nevertheless, MALDI-TOF measurements ($n = 6$ derivative) showed spectra dominated by peaks periodically separated by $m/z \sim 80-84$ units, suggesting fractions made by alternate coupling between hexamethylene and fluoren-9,9-diyl units with molecular masses of 84 and 164, respectively. Absorbance spectroscopy showed a typical fluorene molecule absorbance 266 (ben-
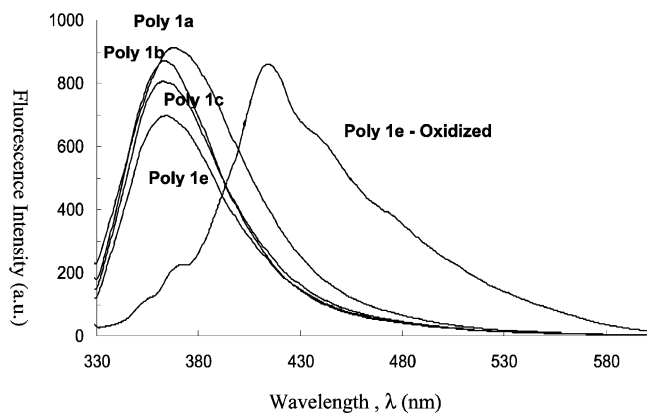
Figure 3. Photoluminescence spectra of solutions of the polymers **1a**−**e** and soluble oxidized derivative of polymer **1e**.
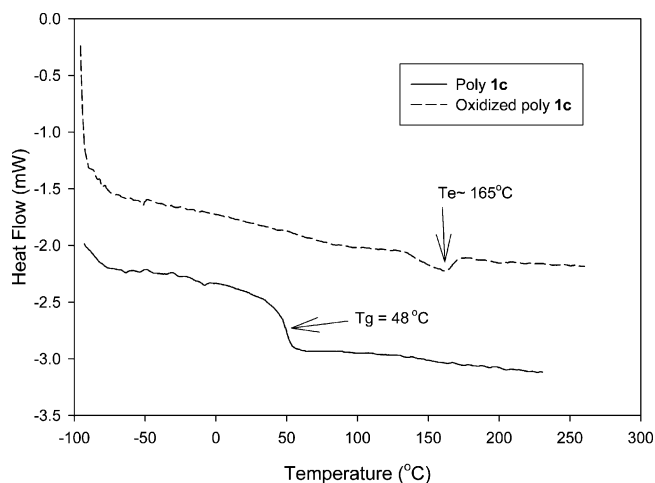

Figure 4. Differential scanning calorimetry (DSC) traces of (solid trace) poly**1c** as polymerized and (broken trace) after chemical oxidation. Notice the near complete disappearance of the $T_g = 48.4$ °C upon oxidation and the appearance of an exothermic transition, T_e, around 165 °C. Heating rate, 10°/min; sample weights, ~5.7 mg.

zenoid) and shoulders at 290 and 301 nm (Figure 2). Finally, thermal analysis (DSC) traces ($n = 8$) showed a distinctive glass transition (T_g) which decreases monotonically as the alkyl chain linker becomes longer and the fluorene content becomes depleted (Figure 4). Again, details of the characterization have been previously reported[22] and are also included in the Supporting Information.

Chemical Oxidation. Oxidation of polymers **1** with FeCl₃ resulted in the formation of insoluble powders for all the polymers except polymer **1e**. The soluble fraction of oxidized polymer **1e** showed, surprisingly, molecular weights close to the parent precursor. On the other hand, the absorbance spectrum of oxidized polymer **1e** (Figure 2) showed a new strong broad absorbance peak around 375 nm, which is in the same range of dialkylfluorenes.[23] This absorbance was found to be consistent to that of poly(dihexylfluorene).[24] This λ_{max} is slightly shorter than λ_{max} for polyfluorenes with controlled molecular weight in which a $\lambda_{max} = 380$ nm is expected. Polymer **1e** also showed absorbances at 266, 294, and 304 nm, which implies that the resulting polymer still has the characteristics of the fluorene group from the unoxidized parts of the polymer. The above results indicate that the oxidation of the polymer gave partially oligomerized fluorene units in the network. Figure 3 shows the representative emission spectrum of the precursor polymers (polymer **1a**−**e**) in CHCl₃ solutions with the same concentrations excited at 300 nm and the emission spectra of the soluble fractions of the chemically oxidized precursor. The un-cross-linked precursors polymers have a fluorescence at 370 nm consistent with fluorene units. The cross-linked and oxidized polymer **1e** has an emission peak at 420 nm. The intensity of fluorescence is actually 10−15 times stronger than that of unoxidized polymer but is shown in Figure 3 on a normalized scale. It is apparent that the oxidative coupling between fluorene units results in emission spectra that are in general agreement with other poly(9,9-dialkylfluorenes).[24] DSC further revealed the striking differences between the precursor polymer and cross-linked derivative. Representative

thermal analysis (DSC) traces before and after chemical oxidation were recorded after an initial conditioning scan as shown in Figure 4. A distinctive T_g is observed with the precursors which decrease monotonically as the alkyl chain linker becomes longer and the fluorene content becomes depleted (see Supporting Information). Chemical oxidation of polymer **1c** resulted in the near disappearance of T_g at the original temperature, but a small endothermic transition (T_e) appeared at higher temperatures. T_e increased as the alkyl linker become longer. We did not attempt to identify the nature of this transition by WAXS, but it may be attributed to a new T_g value with the modified structure of the cross-linked polymer which can have a higher temperature because of greater chain connectivity. The fact that this endotherm value is smaller supports the description of a partially cross-linked polymer. The near complete disappearance of the original T_g though suggests that the oxidative coupling of the fluorene units strongly hinders the mobility of the backbones in the cross-linked derivative.

Electrochemical Oxidation. Figure 5 shows a representative (poly**1c**) CV in methylene chloride, a solvent that also easily dissolves polymers **1**. The electrodeposition in these conditions resulted in robust and transparent films. Film thickness increased monotonically (but sublinearly) with each CV cycle for at least 20 cycles, as shown in the inset of Figure 5 for poly**1c** and -**1d**. Major oxidation events are evident at +1300 and +1600 mV against Ag/AgCl (baseline extrapolated). These events were attributed to fluorene group anodic oxidative coupling and are consistent with the results recently reported by Hapiot et al. in which they suggested the use of higher positive potentials.[16] The first cycle typically showed an earlier oxidation onset at around +1300 mV for polymer **1c**, and this onset shifted toward lower potentials (+1000 mV) after several cycles, suggesting oxidation to form conjugated species, i.e. indicative of fluorene coupling via radical cation generation. The mechanism of this electropolymerization was also recently described as being different from that of other conjugated polymers such as polypyrroles and polythiophenes, in that it required the formation of higher oxidation state intermediates.[16] Note that

(23) Teetsov J.; Vanden Bout, D. *Langmuir* **2002**, *18*, 897; Blondin, P.; Bouchard, J.; Beaupupre, S.; Belletete, M.; Durocher, G.; Leclerc, M. *Macromolecules* **2000**, *33*, 5874.
(24) (a) Inbasekaran, M.; Woo, E.; Wu, W.; Bernius, M.; Wujkowski, L. *Synth. Met.* **2000**, *111−112*, 397. (b) Brizius, G.; Kroth, S.; Bunz, U. H. F. *Macromolecules* **2002**, *35*, 5317.
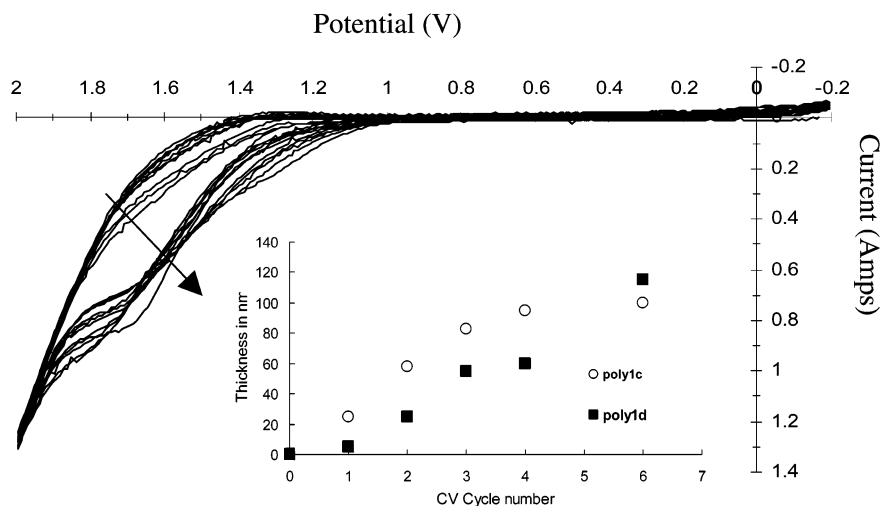
Figure 5. Cyclic voltammetry of poly**1c** in CH$_2$Cl$_2$. Scan speed, 200 mV/s; Ag/AgCl electrode for reference. Solution, 50 mM precursor polymer and 100 mM Bu$_4$NBF$_4$ in methylene chloride; scan, −200 to 2000 mV. Included is the plot of thickness increase with CV cycle for poly**1c** and poly**1d**.
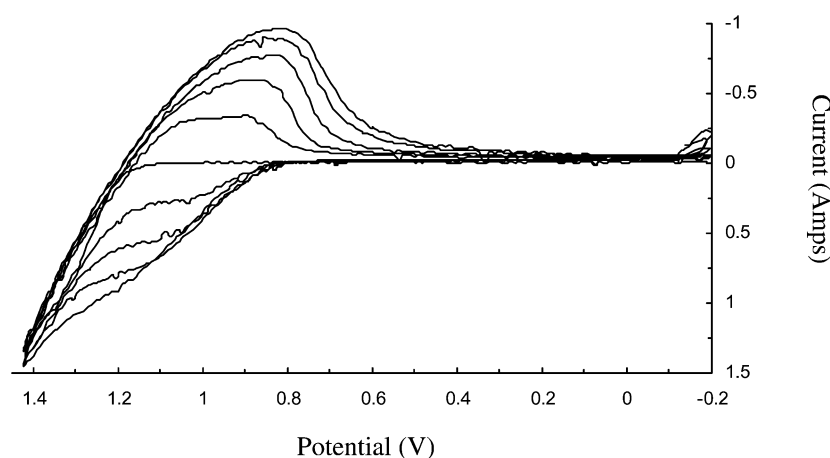

Figure 6. Cyclic voltammetry of poly(*N*-vinylcarbazole) in CH$_2$Cl$_2$. Scan speed, 200 mV/s; Ag/AgCl electrode for reference. The first 5 scans are shown.

the CV's wave amplitudes are relatively independent of the number of cycles which suggests that the electrochemical behavior is not as well behaved compared to other conducting polymers such as polypyrroles and polythiophenes. Nevertheless, CV cycling resulted in increasing film deposition. According to an empirical method first proposed by Bredas and co-workers[25] and modified by Bässler's group,[26] the ionization potentials (IPs) can be estimated from the onset of oxidation potentials by assuming that the energy level of the ferrocene/ferrocenium is 4.8 V below the vacuum level. Since Ag/AgCl has a potential estimated at 435 mV against the ferrocene half-wave potential,[27] one can approximate the IP (eV) = E_{ox} (V) + 4.45 V. All precursor polymers **1** (except poly **1a**) showed similar oxidation events with baseline extrapolation at E_{ox}= 1300 mV, suggesting an IP $\sim$ 5.75 eV for the individual fluorene group (the potential was 5.9 eV for polymer **1a**).[16] The oxidative process observed in the first cycle (IP $\sim$ 5.75) was attributed to (preformed) dimers of fluorene, and the shift toward lower potentials in subsequent scans (IP $\sim$ 5.52 eV) was attributed to the formation of longer oligomeric species.[16] Poly**1d** showed slightly larger values for the oxidation onsets of the third and latter cycles (E_{ox}= 1.2 and 1.17 V) corresponding to IP $\sim$ 5.65 eV. These ionization potentials are thus lower than (by approximately 200 mV) the IP values estimated by

Bradley and co-workers from spin-cast poly(dialkylfluorenes) (IP $\sim$ 5.8 eV).

Electrodeposition of Poly(*N*-vinylcarbazole). To verify the generality of electrooxidative coupling from precursor polymers and to demonstrate the feasibility of using electrochemical deposition as a "directed patterning" method, we also investigated the deposition of another "precursor" polymer, poly(*N*-vinylcarbazole) (PVK).[18a] The carbazole units in PVK can be oxidatively coupled at the 3,6 (or 2,7) positions to yield an electropolymerized poly(alkylcarbazole)-like polymer backbone (ED-PVK).[28] The first CV trace from PVK solution showed a single oxidation event baseline extrapolated onset at +1200 mV which indicated no deposition (Figure 6). On subsequent scans the steady growth of an oxidative event at a lower potential ($E_{ox} \sim$ 850 mV) was observed. The CV of ED-PVK film in a solution without PVK (equivalent to monomer free) shows a broad polymer redox at E_{ox} = 850 mV, and this is attributed to the oxidative formation of carbazole dimers or oligomers during film

(25) Bredas, J. L.; Silbey, R.; Bordeaux, D. S.; Chance, R. R. *J. Am. Chem. Soc.* **1983**, *105*, 6555.
(26) Pommerehne, J.; Vestweber, H.; Guss, W.; Mahrt, R. F.; Bassler, H.; Porsch, M.; Daub, J. *Adv. Mater*. **1995**, *7*, 551.
(27) Janietz, S.; Bradley, D. D. C.; Grell, M.; Giebeler, C.; Inbasekaran, M.; Wu, E. *Appl. Phys. Lett.* **1998**, *73*, 2453.
(28) Ambrose, Nelson *J. Electrochem. Soc.* **1968**, *115*, 1159.

Table 2. EL Performances of Devices Made with Electrodeposited (ED) HT Layers

HT material	HT layer thickness (nm)]	total thickness (nm)	V_{bias} (V) (E^a)	J (mA/cm^2)	L (Cd/m^2)	L/J (Cd/A)
none		85[b]	15.8 (1.9)	100	701	0.7
poly**1b**	35	120	25.3 (2.1)	10.2	121	1.19
poly**1b**	100	185	26.9 (1.4)	3.3	238	0.72
poly**1c**	25	110	14.8 (1.3)	10.5	151	1.44
poly**1c**	100	185	27.9 (1.5)	10.2	44.7	1.1
poly**1d**	5	90	14.0 (1.5)	105	997	0.95
poly**1d**	55	140	23.0 (1.6)	10.1	86	0.85
EP-PVK[c]	110	195	25.8 (1.3)	10.3	130	1.26
EP-PVK[c]	410	495	50.5 (1.0)	1.01	12	1.18

[a] E = average field in 10^6 V/cm. [b] Single layer device with BTF8. [c] EP−PVK = electrooxidized poly(9-vinylcarbazole).

deposition. When compared with that of poly(*N*-ethylcarbazole),[29] the lack of redox peaks at $E_{ox} = 550$mV indicates that ED-PVK contains oligo(carbazol-3,6-yl) species, rather than high polymer. The corresponding ionization potentials observed in this process are IP $\sim$ 5.6 eV and IP $\sim$ 5.25 eV for PVK and EP−PVK, respectively. The value IP $\sim$ 5.8 eV which is often quoted for un-cross-linked PVK[30] is 200 mV higher than our estimate. On the other hand, Wurthner and co-wokers[31] have reported the PVK oxidation potential to be +0.77 V against ferrocene, (corresponding to IP $\sim$ 5.57 eV), which is in closer agreement with our results. The CV's during PVK deposition also show a rapid charge recovery (reduction) during the cathodic cycle, suggesting high charge mobility in the film. We have previously reported the use of cross-linked and electrodeposited PVK to modify work functions and hence hole-transport properties in PLED devices.[32]

Charge Transport Characterization. Our initial motivation was the utilization of these materials to comprise the entire structure of PLEDs. Single-layer devices as well as devices with polymers **1** acting as luminescent or electron transport (EL) layers were fabricated. As described below, these devices showed low efficiencies and short lifetimes (possibly due to premature shorting failures). However, their performance as hole transport materials were found to be much more interesting.

The behavior of a PLED fabricated with the chemically oxidized polymer **1c** as the emissive layer with a thermosetting triarylamine as hole-transport layer (BCB-TPA, IP $\sim$ 5.2 eV, ca. 100 nm)[33] was investigated. The turn-on voltage of this device was near 10 V ($E \sim$ 1 MV/cm), and the rapid rise of the J−V curve at the onset of bias was characteristic of "leaky" devices. The bluish-white light output was low (0.1 Cd/m^2 at 17 V (J = 0.1 mA/cm^2), resulting in device efficiency of the order of $L/J \sim$ 0.1 Cd/A, roughly a decade less efficient than comparable devices made from an efficient polyfluorene-based PLED. The results are shown in the Supporting Information. We thus hypothesize that their low EL efficiency and high bias were the result of low PL efficiency for a cross-linked material.
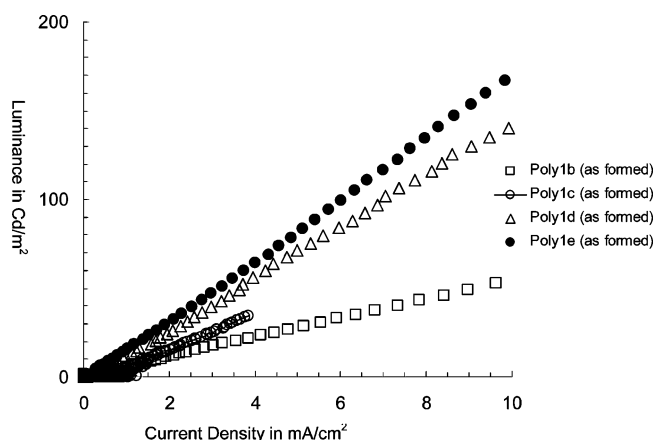
(29) Zotti, G.; Schiavon, G.; Zecchin, S.; Groenendaal, L. *Chem. Mater.* **1999**, *11*, 3624.
(30) Tian, H.; Zhu, W.; Elschner, A. *Synth. Met.* **2000**, *111−112*, 481.
(31) Wurthner, F.; Yao, S.; Schilling, J.; Wortmann, R.; Redi-Abshiro, M.; Mecher, E.; Gallego-Gomez, F.; Meerholtz, K. *J. Am. Chem. Soc.* **2001**, *123*, 2810.
(32) Baba, A.; Onishi, K.; Knoll, W.; Advincula, R. C. *J. Phys. Chem. B* **2004**, *108*, 18949.
(33) Roitman, D. B.; Antoniadis, H.; Hueschen, M.; Moon, R.; Sheats, J. *IEEE J. Sel. Top. Quantum Electron.* **1998**, *4*, 58.
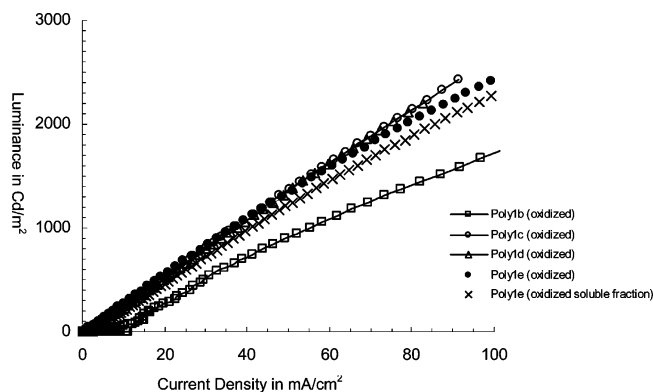
Figure 7. Relation between current density and luminance of light-emitting diodes with poly**1** (polymers as formed or without oxidation) as HT and BTF8 as an EL layer.

Hole injection and charge transport characteristics of polymers **1** were then investigated by fabricating two-layer devices with structure ITO/HT/BTF8/Ca, where polymer **1** which serves as a hole transport (HT) was deposited by either spin-casting and chemical oxidation (Table 1) or by electropolymerization (Table 2). BTF8 has been previously shown to be an excellent EL material with emission centered at 550 nm and estimated IP $\sim$ 5.8 V.[21] BTF8 polymer films were spin-cast over the HT layers from ca. 5% xylene solutions at 2000 rpm.

Spin-cast precursor polymer **1** films were oxidized using a solution of FeCl$_3$ in chlorobenzene. Chlorobenzene is a good solvent for polymer **1**, and it was used to ensure that the entire cross-section of the films would be exposed to the oxidizing reagent. Unfortunately, the precursor fluorene polymer layers became thinned out to ca. 2.5−35 nm by chlorobenzene or xylene (in the case of the unoxidized precursors). The thickness of the HT layers was estimated by subtracting the total device thickness to the thickness of single-layer BTF8 which is typically 85 nm, as obtained using profilometry. The single-layer BTF8 device (first entries in Tables 1 and 2) showed noisy (current leaks) characteristics at low current density (ca. 10 mA/cm^2), but it behaved reproducibly at higher currents (ca. 100 mA/cm^2). Relationships between current density (mA/cm^2) and luminance (Cd/m^2) showed nearly linear behavior or slight sublinear behavior in the range investigated (Figures 7 and 8). Device efficiencies (L/J) of devices with *spin-cast* polymers **1** serving as HT layers were generally higher than the efficiency of a single-layer BTF8 device (0.7 Cd/A) or without polymer **1**, and *increased* in the order **1b** > **1c** >

Figure 8. Relation between current density and luminance of light-emitting diodes with poly**1** (oxidized) as HT and BTF8 as an EL layer.

Figure 9. Thickness (nm) dependence of electrochemically deposited polymer **1** (*C* = spacer alkyl chain length) and polycarbazole HT layer on device efficiency (Cd/ A).

1d > **1e.** Notably, both unoxidized, i.e., precursors (Figure 7), and chemically oxidized polymers **1** (Figure 8) showed this trend. The *chemically* oxidized HT layers showed higher efficiencies as well as lower operating bias (lower field strength) than the *unoxidized* materials and the single-layer device. The best materials were oxidized **1d** and oxidized **1e** with 2.3 and 2.4 Cd/A, respectively, at ~100 mA/cm², and low bias (less than half the field strength than the single layer BTF8 device) as shown in Table 1. The film thicknesses were rather difficult to estimate (especially for the unoxidized samples), but this parameter did not appear to be a strong factor in the performance of these devices. It appears that thin layers (35 nm or less) of polymer **1** films, especially in the oxidized form, enhanced both carrier injection and electroluminescence efficiency relative to the single-layer device. An unexpected result was that the best device performances were observed with polymer **1** with the longest alkyl links (C10 and C12) even without oxidation.[34] We propose that the role of the HT layer in this case is very similar to the devices with self-assembled ultrathin "interlayers" considered by Greenham and co-workers.[35] These authors observed that polymeric layers (formed on ITO by sequential adsorptions of polyelectrolyte and ionomers of opposite charge) of the order of 1−16 nm result in enhanced efficiency and, in the case of conducting polymer interlayers, enhanced carrier injection relative to single-layer MEH−PPV devices. They attributed this effect primarily to the role of the interlayer in blocking electrons from leaving the emissive polymer, thus reducing their leakage into the anode contact. It is believed that the majority carriers in MEH−PPV are holes, but for polyfluorene-based devices the majority carriers are usually electrons due to difficulties in injecting holes in polyfluorenes using conventional architectures.[20,21] Therefore blocking electrons very close to the anode (within a few nanometers) probably results in redistributing the electric field to enhanced hole injection from ITO into the EL layer and is specific for polyfluorenes.[20,21]

Table 2 shows the behavior of two-layer devices fabricated by the electrodeposition of polymers **1** or ED-PVK on ITO as HT layers followed by spin-casting BTF8. Device efficiencies and field strengths necessary to drive the devices
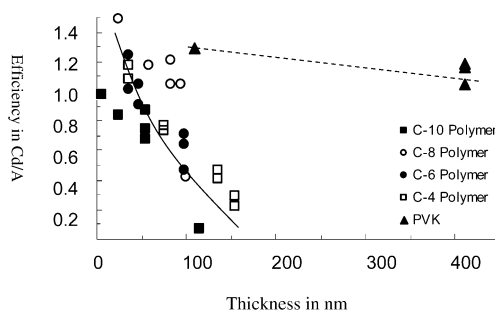
to ca. 10 mA/cm² are shown for two different film thicknesses for each polymer. Note: ED-polymer **1b** (100 nm) and ED-PVK (410 nm) devices shorted before reaching this current density. Electrodeposited films were typically thicker than in chemically oxidized devices and were measured with higher accuracy since solvent erosion was negligible in this case. This is a consequence of the insolubility produced by network formation (cross-linking) with CV. All devices with a HT layer showed higher efficiency than the single-layer BTF8 device. Thinner HT layers resulted in higher efficiencies (ca. 1.44 Cd/m² for 2.5 nm ED-polymer **1c**), but not nearly as high as with the devices fabricated by chemical oxidization (Figure 9). Thicker HT films (ca. >10.0 nm) resulted in substantially lower PLED efficiencies, although their current density field dependence (*E*) remained relatively independent of thickness (*E* ~ (1.3−1.6) × 10⁶ V/cm at 10 mA/cm²). In contrast with the chemically oxidized polymers **1**, PLED performances in this case were independent of alkyl chain length. The combination of independence of field strength with HT thickness and strong dependence in device efficiency with thickness suggests that the majority charge carriers (electrons) are not transport-limited through the bulk of the "HT" film, but the minority carriers (holes) are transport-limited, resulting in an imbalance of charge recombination in the BTF8 layer. In other words, these devices are less dominated by energy barrier tunneling between layers and appear to be controlled by charge-transport limitations throughout their HT films. Thus, electron mobility appears to be relatively high in polymers **1** and hole mobility rather low (but not lower than in BTF8) for these films. On the basis of these results, one can also attribute the low efficiency of the single-layer polymer **1c** (as emitting layer) primarily to the low PL efficiency of polymer **1**, and not to its charge transport or injection characteristics. It is clear that the network formation influences the mechanical/thermal and hole-transport properties of these films. Other groups have also reported strategies for more efficient hole-transport materials (and high charge carrier mobility) using conjugated organometallic polymer networks.[36]

Devices with ED-PVK as HT layers behaved substantially different. As shown in Table 2, the field dependence is lower (~1.3 × 10⁶ V/cm for *J* ~ 10 mA/cm²), and there is virtually no quantum efficiency dependence (ca. *L/J* ~ 1.2 Cd/A) on film thickness. Note: the ED-PVK 41.0 nm thick device was

(34) Yanagi, H.; Okamoto, S. *Appl. Phys. Lett.* **1997**, *71*, 2563.
(35) Ho, P. K. H.; Granstrom, M.; Friend, R. H.; Greenham, N. *Adv. Mater.* **1998**, *10*, 769.

(36) Kokil, A.; Shiyanovskaya, I.; Singer, K. D.; Weder, C. *J. Am. Chem. Soc.* **2002**, *124*, 9978.
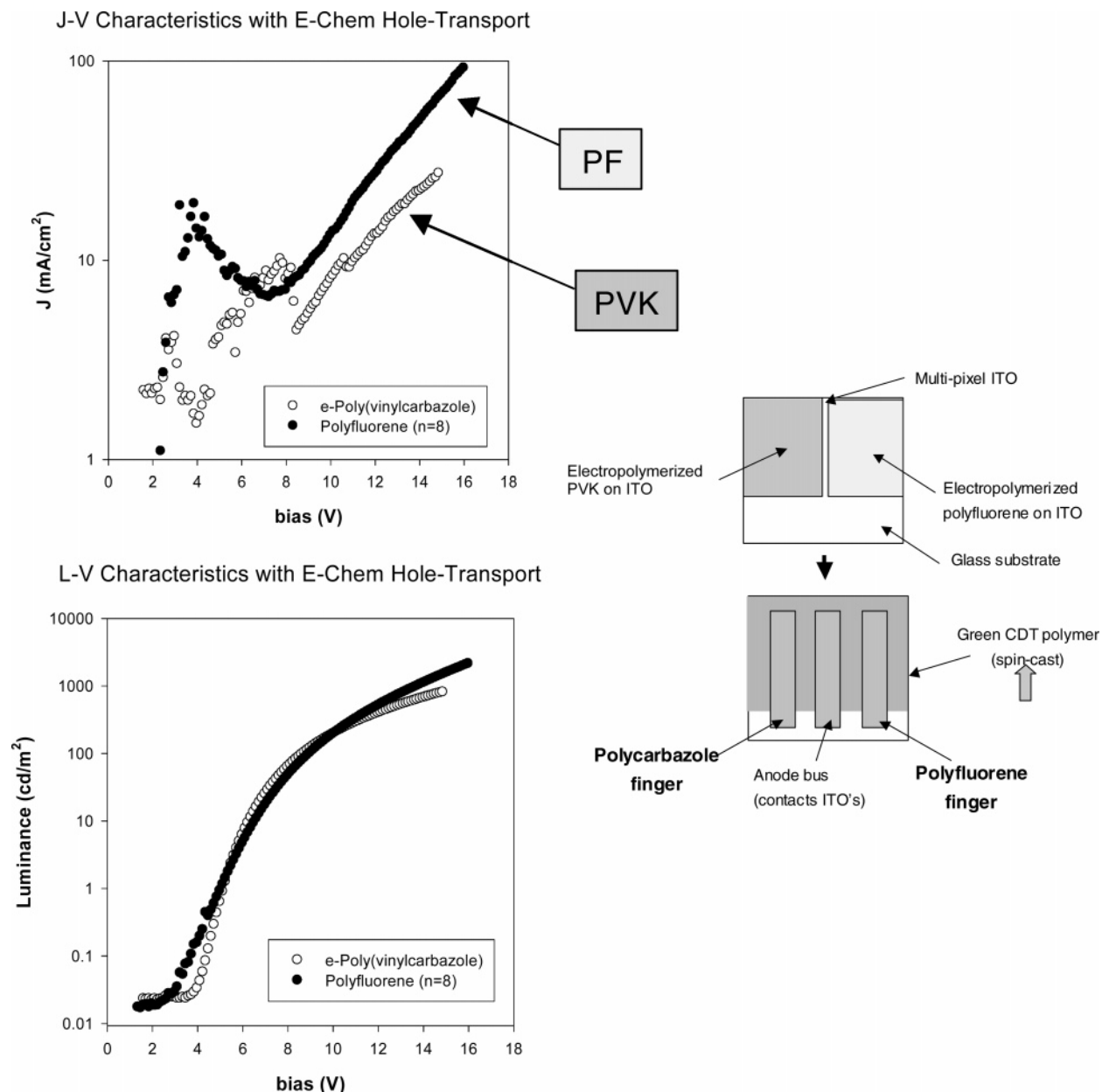
Figure 10. Device performance of multipixel light-emitting diode with poly**1c** and PVK as HT layers (structure of the device is shown above) showing $J-V$ and $L-V$ characteristics.

run only to 1.01 mA/cm^2 due to the high bias required, 50.5 V, but light output was nearly linear with current density in this range. Luminance losses by film absorbances were not considered in this case. This behavior suggests that the ED-PVK HT layer is capable of supplying sufficient minority carriers (independent of thickness) to maintain charge recombination constant in the EL layer. It is somewhat surprising, however, that the low IP $\sim$ 5.25 V estimated for this material did not result in substantially higher hole injection resulting in much higher efficiencies. A possible explanation for this is that this polymer might not be a very effective electron-blocker, allowing the electrons to escape the EL layer without recombination. Recently, we have also demonstrated work-function tunability of electrodeposited PVK HT layers with polyfluorene EL polymers based on selective doping.[32]

In summary, charge injection behavior and transport characteristics of the films were found to be a complex

contribution of the EL and HT layers and showed interesting thickness and polymer dependence. Spun-cast precursors and chemically oxidized, hole-transport layers resulted in very thin HT films (typically less than 35 nm) due to solvent erosion either during the oxidation step or by the deposition of the EL layer (BTF8). However, their presence next to ITO in ITO/HT/BTF8/Ca PLEDs resulted in considerable performance enhancement (both in efficiency and luminance) relative to the single-layer ITO/BTF8/Ca. The enhancements were largest for the oxidized (and un-oxidized) polymers with highest alkyl contents (C12), and the behavior was relatively independent of HT thickness. We attributed this result to interfacial energy barriers, partially blocking electrons from leaving the emissive polymer and resulting in increased hole injection by the local field enhancement near the anode. Electrodeposition allowed for the investigation of thicker films. In this case, however, the efficiency of the devices showed only modest improvements over single-layer BTF8

Cross-Linked Polyfluorene Polymer Precursors

Chem. Mater., Vol. 17, No. 26, 2005 **6789**

devices (approximately 1.5−2 times). Device efficiencies were weakly dependent on alkyl lengths, but they were strongly dependent on HT thickness, and this was attributed to hole-transport limitations across the bulk of the HT films, affecting charge balance in the EL layer. Quantum efficiency increased for thinner HT layers, but the behavior did not quite approach the observed chemically oxidized "interlayer" performances. It is unclear at this time whether the differences in behavior were due to a lower degree of oxidative coupling in ED films, to different molecular architectures, or to the presence of dopants (i.e. remnant Fe^{3+} ions) in the chemically oxidized "interlayers". Finally, poly(carbazole) (ED-PVK) with low IP $\sim$ 5.25 V was also investigated. The quantum efficiencies and field dependences of devices made with the structure ITO/ED-PVK/BTF8/Ca were modestly higher than the single-layer device (1.2 Cd/A vs 0.7) and nearly independent of ED-PVK thickness. This suggests that ED-PVK has better charge-transport characteristics for both holes and electrons (compared to BTF8), but in a HT layer, it does not improve very substantially the charge balance of BTF8. In a future work we plan to investigate electrodeposited copolymers of PVK with conducting polymers known to block electrons more efficiently.

Fabrication of Two-Pixel Device by Electrodeposition. To demonstrate site-directed deposition, a primitive two-pixel PLED was fabricated by the sequential electrodeposition of PVK and polymer **1c** on an ITO-patterned substrate containing two unconnected regions ("pixels") as illustrated in Figure 10. The electrodeposited polymer films were used as differentiated HT layers, having a common EL layer (BTF8). Each pixel was addressed independently by a corresponding cathodic layer patterned using a shadow mask during evaporation. Figure 10 shows the separate J−V (a) and L−V (b) characteristics of the two-pixel device. These showed that the original characteristics of the devices were retained after this multistep fabrication approach, but the performance is rather "leaky" for the J−V characteristics. The measurements of the L−V properties were more reproducible and showed comparable behavior indicating the major role of the BTF8 polymer in defining the device luminescence performance predominates. The luminance behavior is nearly the same, highlighting the role of polymer **1** and PVK as simply HT layers. Nevertheless, the fact that the two precursor polymers polymer **1** and PVK showed different J−V characteristics demonstrates the viability of a two-site or even multisite electrodeposition process in the preparation of patterned LED devices. Further work is in progress to optimize the pixilated device characteristics of these materials. Recently, electrochemical micropatterning and even nanopatterning of precursor polymer materials have been demonstrated by our group.[7]

Conclusion

In this work, we have utilized "precursor" fluorene-containing polymers with novel alternating structures. Their unique molecular structures enabled chemical or electrochemical (oxidative) deposition of high-quality films from good solvents. The oxidized films are insoluble due to the formation of three-dimensional network structures corresponding to cross-linked by intramolecular and intermolecular couplings of fluorenyl units. Optically, both chemically oxidized and electrodeposited polymers showed characteristics similar to those of previously reported poly(dialkylfluorenes), but the extent of fluorenyl coupling is probably not very large and nonregiospecific, especially for the electropolymerized materials. PL efficiencies were also observed to be low. However, their properties as hole-transport materials are interesting, demonstrating structure dependence (the extent of alkyl spacer chain length) and thickness independence. Different modes of charge transport were attributed when comparing chemically oxidized and electrodeposited HT layer films. We extended the electrodeposition method to PVK and used this approach to demonstrate a two-side deposition or pixelization of a prototype PLED without using photolithography or inkjet printing.

Supporting Information Available: Word file and PDF of experimental details showing synthesis procedure, NMR, GPC, characterization, modeling of reaction, and PLED device performance of polymer **1**. This material is available free of charge via the Internet at http://pubs.acs.org.

CM051440Y